

# Localised plumes in three-dimensional compressible magnetoconvection

S. M. Houghton<sup>1</sup> \*and P. J. Bushby<sup>2</sup> †

<sup>1</sup> School of Mathematics, University of Leeds, LS2 9JT, UK.

<sup>2</sup> School of Mathematics & Statistics, Newcastle University, Newcastle upon Tyne, NE1 7RU, UK.

Draft prepared October 30, 2018

## Abstract

Within the umbrae of sunspots, convection is generally inhibited by the presence of strong vertical magnetic fields. However, convection is not completely suppressed in these regions: bright features, known as umbral dots, are probably associated with weak, isolated convective plumes. Motivated by observations of umbral dots, we carry out numerical simulations of three-dimensional, compressible magnetoconvection. By following solution branches into the subcritical parameter regime (a region of parameter space in which the static solution is linearly stable to convective perturbations), we find that it is possible to generate a solution which is characterised by a single, isolated convective plume. This solution is analogous to the steady magnetohydrodynamic convectons that have previously been found in two-dimensional calculations. These results can be related, in a qualitative sense, to observations of umbral dots.

## 1 Introduction

Using modern instruments, such as the Solar Optical Telescope on board Hinode and the 1-metre Swedish Solar Telescope on La Palma, it is possible to make detailed observations of magnetic fields and convection at the surface of the Sun. Sunspots are the most prominent magnetic features on the solar surface. A typical sunspot consists of a central umbral region, surrounded by a complex filamentary penumbra. Umbral regions appear dark because their surface temperatures are (typically) only 70 – 85% of the mean surface temperature of the non-magnetic photosphere (see, for example, Thomas & Weiss, 2008). This reduction in temperature is due to the fact that the convective transport of heat is impeded within sunspot umbrae by the presence of strong, near vertical magnetic fields (which can often exceed 3000G).

Detailed observations of sunspot umbrae have shown that they are not uniformly dark. In almost all sunspots, bright point-like structures can be observed – these are known as umbral dots (Danielson, 1964). These bright features are warmer than their immediate surroundings, but are (generally) cooler than the surrounding photosphere (see, for example, Sobotka & Hanslmeier, 2005; Kitai et al., 2007). It is difficult to determine the characteristic size of an umbral dot, although these features are always small compared to the umbral diameter. In a recent study, Kitai et al. (2007) found that the umbral dots in one particular sunspot had typical diameters of approximately 220 – 350km, although a significant number appeared to be much smaller than this (possibly below the resolution limit for the Solar Optical Telescope on Hinode). Umbral dots are also short-lived features. Kitai et al. (2007) found that most of the umbral dots in their survey had lifetimes of between 5 and 20 minutes. In an earlier study, Sobotka et al. (1997) found a much broader range of lifetimes for umbral dots (with a small percentage lasting longer than 2 hours), although, like Kitai et al. (2007), they found a mean lifetime of approximately 15 minutes. Most umbral dots exhibit no systematic proper motions. However, those that appear to form at the umbral/penumbral boundary (which are often associated with penumbral grains) tend to migrate radially inwards towards the centre of the umbra (Sobotka et al., 1995; Kitai et al., 2007). There is some observational evidence for weak upflows within umbral dots (Socas-Navarro et al., 2004; Bharti et al., 2007) as well as downflows around their edges (Bharti et al., 2007; Ortiz et al., 2010). Clearly, the observations indicate that umbral dots correspond to convective plumes

---

\*Email: smh@maths.leeds.ac.uk

†Email: paul.bushby@ncl.ac.uk

within sunspot umbrae. Further theoretical support for this conclusion comes from the work of Deinzer (1965), who determined that convective motions must be present within the umbra, as radiative processes alone could not transport sufficient energy to the surface.

Theoretical studies of umbral convection tend to be based upon local models of magnetoconvection in a Cartesian domain. It is well-known that a strong vertical magnetic field tends to inhibit convective motions in an electrically-conducting fluid (Chandrasekhar, 1961). When the dynamics are dominated by magnetic fields, convection takes the form of weak, narrow plumes. In an idealised model of magnetoconvection, Weiss et al. (2002) found a steady, almost hexagonal pattern of convection in the magnetically-dominated regime. More recently, Schüssler & Vögler (2006) (see also Bharti et al., 2010) have carried out a more realistic set of calculations, including the effects of partial ionisation and radiative transfer. These simulations produced a time-dependent pattern of individual convective plumes, the properties of which compare very favourably to observations of umbral dots. In the calculations of Weiss et al. (2002) and Schüssler & Vögler (2006), convective features tend to be distributed across the whole computational domain. It is worth noting that observations indicate that the distribution of umbral dots tends to be rather non-uniform (Sobotka & Hanslmeier, 2005). This could simply be explained by variations in intensity (as seen in the calculations of Schüssler & Vögler, 2006), but some degree of localisation in the distribution of convective plumes could also help to explain the observed distribution of umbral dots.

In a two-dimensional model of incompressible magnetoconvection, Blanchflower (1999) found strongly localised, steady convective states (see also Dawes, 2007). These were named convectons. Restricting attention to a simplified model, in which the governing equations were projected onto a minimal set of Fourier modes in the vertical direction, Blanchflower & Weiss (2002) were also able to find oscillatory localised states in three spatial dimensions. In both these cases, these localised states were found in the subcritical parameter regime (in which the static, purely conducting state is linearly stable to convective perturbations). These localised states are an extreme example of a phenomenon that is known as flux separation (Tao et al., 1998). Convective plumes tend to expel magnetic flux (Weiss, 1966), causing it to accumulate in the surrounding fluid. In this subcritical parameter regime, the magnetic field that surrounds the plume becomes sufficiently strong that convection in the surrounding fluid is completely inhibited, giving rise to a truly localised convective state. If conditions are appropriate for subcritical convection within sunspots (something that is certainly plausible), these results suggest that it may be possible for truly localised umbral dots to form within sunspot umbrae.

In this paper, we demonstrate the existence of steady localised convective plumes in three-dimensional compressible magnetoconvection. Unlike Blanchflower & Weiss (2002), we make no simplifying assumptions regarding the vertical structure of the convective flows. The setup of the model is described in detail in the next section of the paper. Numerical results from this model are presented in Section 3. In the final section, we relate our findings (in qualitative terms) to observations of umbral dots.

## 2 Problem description and setup

We consider the evolution of a layer of compressible, electrically-conducting fluid, heated from below, in the presence of an imposed magnetic field. Various properties of the fluid, including the thermal conductivity,  $K$ , the shear viscosity,  $\mu$ , the magnetic diffusivity,  $\eta$ , the magnetic permeability,  $\mu_0$ , and the specific heat capacities at constant pressure and density ( $c_P$  and  $c_V$  respectively) are assumed to be constant. At a position  $\mathbf{x}$  and time  $t$ , we define  $\rho(\mathbf{x}, t)$ ,  $T(\mathbf{x}, t)$  and  $\mathbf{u}(\mathbf{x}, t)$  to be the fluid density, temperature and velocity field (respectively), whilst  $\mathbf{B}(\mathbf{x}, t)$  represents the magnetic field.

This fluid occupies a three-dimensional Cartesian domain with  $0 \leq z \leq d$  and  $0 \leq x, y \leq 8d$ . The axes of this coordinate system are orientated so that the  $z$ -axis points vertically downwards, parallel to the constant gravitational acceleration,  $\mathbf{g} = g\hat{\mathbf{z}}$ . For this model problem, periodic boundary conditions are imposed in the  $x$  and  $y$  directions, whilst the upper and lower boundaries (at  $z = 0$  and  $z = d$ ) are assumed to be impermeable and stress free. Furthermore, fixed temperature boundary conditions are applied at the upper and lower boundaries with  $T = T_0$  at  $z = 0$  and  $T = T_0 + \Delta T$  at  $z = d$  ( $\Delta T > 0$ ). It is also assumed that the horizontal components of any magnetic fields that are present vanish at  $z = 0$  and  $z = d$ . When the layer is static, the imposed magnetic field is uniform and vertical, i.e.  $\mathbf{B} = B_0\hat{\mathbf{z}}$ .

Before writing down the governing equations for this system, we can express these in non-dimensional form. More details of this procedure can be found in Matthews et al. (1995) and Bushby & Houghton (2005). Very briefly, all lengths are scaled by the layer depth,  $d$ , whilst an acoustic time-scale,  $d/(R_*T_0)^{1/2}$  (where  $R_*$  is the gas constant) is used to rescale time. After rescaling  $\rho$ ,  $T$ ,  $\mathbf{u}$  and  $\mathbf{B}$  in an appropriate way (see

Parameter	Definition	Values used
$\gamma$	$c_P/c_V$	5/3
$m$	$gd/R_*\Delta T - 1$	1.0
$\theta$	$\Delta T/T_0$	10.0
$\kappa$	$K/\rho_0 dc_P(R_*T_0)^{1/2}$	0.2
$\zeta_0$	$\eta\rho_0 c_P/K$	0.1
$\sigma$	$\mu c_P/K$	1.0
$F$	$B_0^2/\rho_0\mu_0 R_*T_0$	Variable

Table 1: The non-dimensional parameters in the governing equations for compressible magnetoconvection. Note that  $\rho_0$  corresponds to the unperturbed density at the upper surface of the layer. All other parameters are as defined in the text.

Bushby & Houghton (2005) for more details), the governing equations for this system can be written in the following form:

$$\frac{\partial \rho}{\partial t} = -\nabla \cdot (\rho \mathbf{u}), \quad (1)$$

$$\begin{aligned} \frac{\partial}{\partial t} (\rho \mathbf{u}) = & -\nabla \cdot (\rho T + F|\mathbf{B}|^2/2) + \theta(m+1)\rho \hat{\mathbf{z}} \\ & + \nabla \cdot (F\mathbf{B}\mathbf{B} - \rho \mathbf{u}\mathbf{u} + \kappa \sigma \boldsymbol{\tau}), \end{aligned} \quad (2)$$

$$\frac{\partial \mathbf{B}}{\partial t} = \nabla \times (\mathbf{u} \times \mathbf{B} - \kappa \zeta_0 \nabla \times \mathbf{B}), \quad (3)$$

$$\begin{aligned} \frac{\partial T}{\partial t} = & -\mathbf{u} \cdot \nabla T - (\gamma - 1)T \nabla \cdot \mathbf{u} + \frac{\kappa \gamma}{\rho} \nabla^2 T \\ & + \frac{\kappa(\gamma - 1)}{\rho} (\sigma \tau^2/2 + F\zeta_0 |\nabla \times \mathbf{B}|^2), \end{aligned} \quad (4)$$

where the components of the stress-tensor,  $\tau$ , are given by

$$\tau_{ij} = \frac{\partial u_i}{\partial x_j} + \frac{\partial u_j}{\partial x_i} - \frac{2}{3} \frac{\partial u_k}{\partial x_k} \delta_{ij}, \quad (5)$$

whilst  $\mathbf{B}$  satisfies the standard constraint that  $\nabla \cdot \mathbf{B} = 0$ . The pressure  $P$  satisfies

$$P = \rho T. \quad (6)$$

Equation (1) describes the conservation of mass, whilst Equation (2) is simply the momentum equation, written in conservative form. Note that the  $\theta(m+1)\rho \hat{\mathbf{z}}$  term in Equation (2) represents the effects of gravity whilst the two terms that are quadratic in  $\mathbf{B}$  correspond to the Lorentz force. The evolution of the magnetic field is governed by the standard magnetic induction equation (3). The final two terms in the thermal equation (4) represent the effects of viscous and ohmic heating. The non-dimensional parameters that appear in the governing equations are defined in Table 1. For later convenience, we also introduce the Chandrasekhar number,

$$Q = F/\kappa^2 \zeta_0 \sigma, \quad (7)$$

and the Rayleigh number,

$$Ra = (m+1 - m\gamma)(1 + \theta/2)^{2m-1} \frac{(m+1)\theta^2}{\kappa^2 \gamma \sigma}. \quad (8)$$

The Chandrasekhar number is a measure of the strength of the imposed magnetic field whilst the Rayleigh number measures the destabilising influence of the temperature gradient that is imposed across the layer. If all other parameters are fixed, varying  $Ra$  and  $Q$  is equivalent to varying  $F$  and  $\kappa$ .

There is a non-trivial equilibrium solution to these governing equations, corresponding to a static polytropic layer with a uniform, vertical magnetic field:

$$\mathbf{u} = 0, \quad T(z) = 1 + \theta z, \quad \rho(z) = (1 + \theta z)^m, \quad \mathbf{B} = \hat{\mathbf{z}}. \quad (9)$$

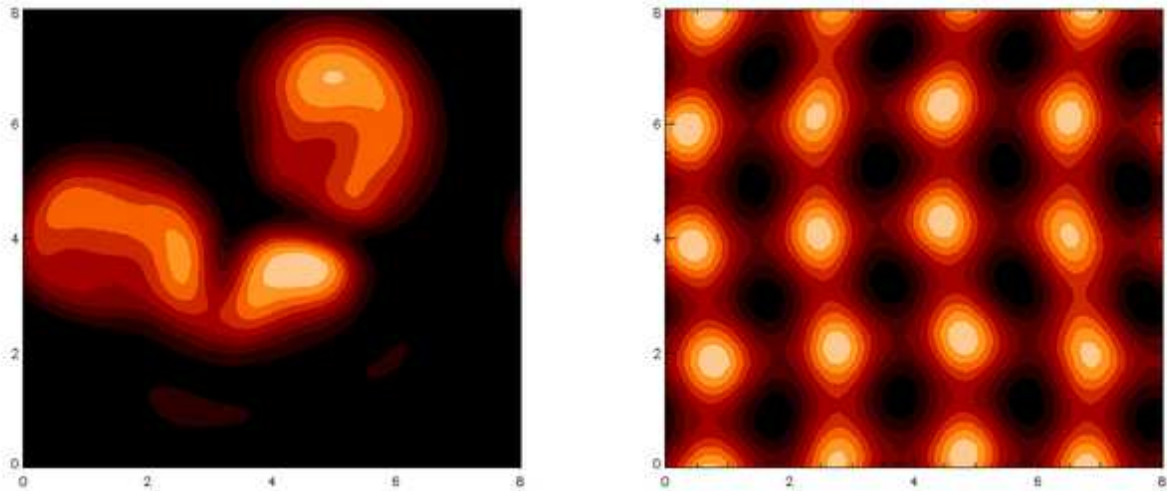


Figure 1: The temperature distribution in a horizontal plane just below the upper surface of the computational domain for  $Q = 120$  (top) and  $Q = 150$  (bottom). Brighter contours correspond to regions of warmer fluid. These simulations were both evolved from a static state.

In this equilibrium state, the parameters that are given in Table 1 imply that the layer of fluid is highly stratified, with the temperature and density both varying by a factor of 11 across the depth of the domain. When there is no magnetic field present (i.e. when  $Q = 0$  or, equivalently,  $F = 0$ ), the critical Rayleigh number for the onset of convection in this layer is approximately,  $Ra = 1189$ . For the parameters given in Table 1,  $Ra = 6000$ , hence this layer is convectively unstable in the absence of an imposed magnetic field. As in Boussinesq magnetoconvection (Chandrasekhar, 1961), magnetic fields tend to inhibit convection. Hence, non-zero values of  $Q$  lead to an increase in the critical Rayleigh number. Table 1 also gives values for two diffusivity ratios,  $\sigma$  and  $\zeta_0$ . For simplicity, we set  $\sigma = 1.0$ . The value of  $\zeta_0$  plays a crucial role in determining the near-onset bifurcation structure. As was the case in the truncated Boussinesq model of Blanchflower (1999), a choice of  $\zeta_0 = 0.1$  ensures that the equilibrium state can be unstable to oscillatory modes of convection as well as stationary modes.

### 3 Numerical results

Given the complexity of the governing equations, it is necessary to solve these numerically. We cover the Cartesian domain with a computational mesh, typically consisting of  $128 \times 128 \times 96$  grid points. Using standard Fast Fourier Transform (FFT) libraries, all horizontal derivatives are evaluated in Fourier space. Fourth-order finite differences are used to calculate the vertical derivatives. The temporal evolution of this system is determined by an explicit third-order Adams-Bashforth scheme. This code is parallelised using MPI.

#### 3.1 Supercritical convection

As described in Section 2, one simple solution of these governing equations corresponds to a static polytropic layer in the presence of a uniform, vertical magnetic field (equation 9). We use this static solution (plus a small thermal perturbation) as an initial condition for the code. For the parameter values that are given in Table 1, this initial state is convectively unstable provided that the Chandrasekhar number does not exceed a value of (approximately)  $Q = 160$ . Since this equilibrium solution is unstable when  $Q < 160$ , we refer to this region of parameter space as the ‘supercritical’ parameter regime.

Figure 1 shows snapshots of the system for two different values of  $Q$  ( $Q = 120$  and  $Q = 150$ ), once a statistically-steady state has been reached. Each plot shows the temperature distribution across a horizontal layer, just below the upper surface of the domain. When  $Q = 120$ , the solution is characterised by several time-dependent plumes from which most of the surface magnetic field has been expelled by the convective motions. Elsewhere the flow is dominated by magnetic effects, so much so that the Lorentz force is strong enough to (almost) completely inhibit convection. Solutions of this form are reminiscent of the ‘flux-separated’ states that were found by Weiss et al. (2002) although, in that study, small-scale convective cells tended to

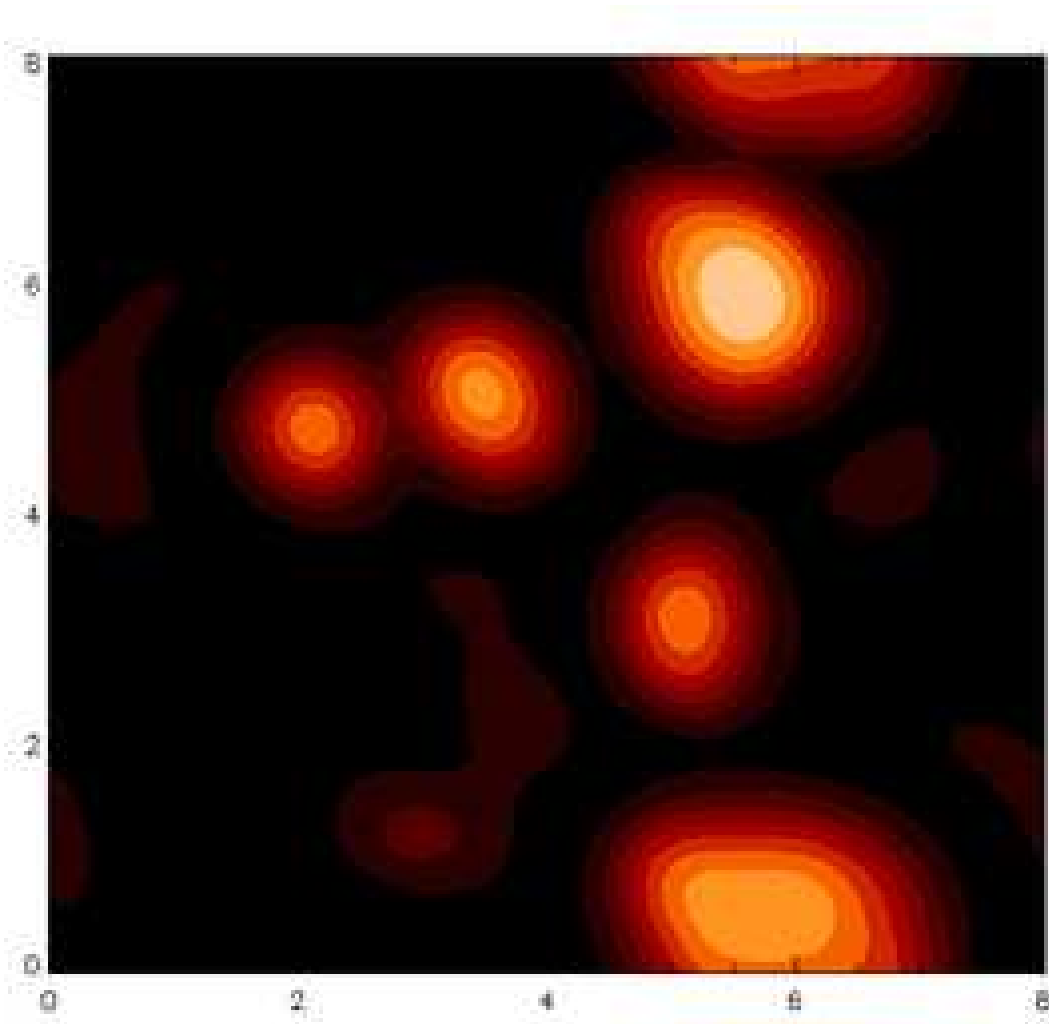


Figure 2: Like the lower part of Figure 1, this shows the temperature distribution, for  $Q = 150$ , across a horizontal layer just below the upper surface of the domain. This solution has been generated by following the flux-separated solution branch.

be found in the magnetically-dominated regions. Here the magnetic suppression of convection is much more pronounced in this flux-separated state. A very different form of solution is found when  $Q = 150$  (lower part of Fig. 1). In this simulation, the convection forms an oscillatory pattern that is distributed across the whole of the domain.

Linear theory (see, for example, Chandrasekhar, 1961) predicts oscillatory convection in the magnetically-dominated regime, at least for low values of  $\zeta_0$ . Hence the oscillatory behaviour of the simulation at  $Q = 150$  is unsurprising. The convection at  $Q = 120$  is also time-dependent, as noted above, but this flux-separated state is representative of a different solution branch. Although the present model is much more complicated than the two-dimensional Boussinesq model that was considered by Blanchflower (1999), it is clearly of interest to relate the two studies. The flux separated state at  $Q = 120$  would correspond to one of the multiple roll states that are shown in the bifurcation diagram in Figure 3 of Blanchflower (1999). The existence of different solution branches raises the possibility that a given set of parameter values could be associated with more than one stable state. Following the procedure that is described by Blanchflower (1999), solution branches can be followed by starting a simulation with fully developed convection, rather than evolving it from a static state. Having adjusted the value of  $Q$ , the simulation can then be evolved again until a statistically-steady state has been found. For example, if the  $Q = 120$  solution is taken as an initial condition, the flux-separated solution branch can be followed by gradually increasing the strength of the the magnetic field (by increasing the value of  $Q$ ). The outcome of such a procedure is illustrated in Figure 2, which shows the temperature distribution for a flux-separated solution at  $Q = 150$ . Comparing this plot with the lower part of Figure 1, it is clear that

(at least) two distinct solutions exist for this set of parameter values. This flux-separated solution has smaller convective plumes than the  $Q = 120$  case. This is a consequence of the fact that magnetic fields are now strong enough to inhibit convection in a larger proportion of the computational domain. The typical scale of convection is reduced by increasing the strength of the imposed magnetic field. Additionally the rate at which convective plumes merge together, and split apart, reduces as the strength of the imposed magnetic field is increased.

### 3.2 The subcritical parameter regime

As noted above, the static polytropic layer is (linearly) stable to convective perturbations for values of the Chandrasekhar number in excess of approximately  $Q = 160$ . Hence, we refer to this range of parameter space as the ‘subcritical’ regime. In order to find non-trivial behaviour in this parameter regime, it is clearly necessary to adopt a non-static initial condition for any simulations that are carried out. Given the results that were presented in the previous section, it is natural to try to track the flux-separated solution branch into this subcritical regime by incrementally increasing the value of  $Q$  (as before, looking for a statistically-steady state before each increment). By following an analogous procedure, Blanchflower (1999) found localised states in a two-dimensional model, so this would appear to be the most sensible approach.

As the value of  $Q$  is gradually increased, following the flux-separated branch, the dynamical influence of the magnetic field becomes greater. This leads to a reduction in both the number and scale of the field-free convective plumes. This process continues until a single steady plume remains. This plume is the three-dimensional analogue of the two-dimensional ‘convecton’ solutions that were found by Blanchflower (1999). This three-dimensional convecton is illustrated in Figures 3 and 4. At  $Q = 215$ , this localised convective plume is almost axisymmetric, being slightly elongated in the  $x$ -direction, with a broad central upwelling, surrounded by a narrow downflow region. Convection is completely suppressed everywhere else by a strong, uniform, vertical magnetic field. The magnetic field distribution within the convecton is more complicated. At the surface, the field is almost completely expelled by the diverging convective flows. Towards the base of the plume, converging convective flows lead to an accumulation of vertical magnetic flux at the base of the convective upflow. The stratification of the layer clearly does play a role in determining the structure of this localised convective feature: slightly larger temperature perturbations are found near the top of the layer. It should be stressed that this convecton is steady and is therefore not simply a transient phenomenon. It is also worth noting that, although the horizontally averaged convective flux is small, the local perturbations to the thermodynamic variables are of order unity within the convecton itself. Therefore this is also a dynamically significant feature, albeit a highly localised one.

It should be noted that this convecton is not truly localised rather, by virtue of the horizontal boundary conditions, it is part of a periodic array of such convective structures. As seen in figure 4 each structure is separated by approximately 6 non-dimensional units which is approximately 3 times the width of the convective structure. Therefore, any influence from neighbouring convectons will be small. An initial investigation in larger computational domains confirms this to be the case. Similar localised states can be found, although the range of  $Q$  for which they exist does change with domain size. Attempts to find an analytic description of a perfectly axisymmetric convecton are ongoing.

Having found this convecton, this solution branch can also be tracked to determine its range of stability. In fact, the solution that is shown in Figures 3 and 4 corresponds to the largest value of  $Q$  at which the convecton is found to be stable. This is also the value of  $Q$  at which the greatest degree of localisation is found. As this solution branch is followed into the weaker field regime (by gradually *decreasing* the value of  $Q$ ), the convecton grows, becoming increasingly asymmetric. For example, at  $Q = 190$  the solution is still highly localised and steady, but the convective cell is about 25% wider than the convecton at  $Q = 215$  and is more elongated in the  $x$ -direction. For this larger localised state, it is plausible that the finite size of the computational domain is (weakly) influencing the symmetry of the convective plume. Reducing  $Q$  still further, we find that the solution is still mostly localised, although there are now weak (but significant) fluctuations elsewhere in the domain. More importantly, the convecton is no longer steady. Instead, the plume ‘wobbles’ periodically about its central axis (as illustrated in Figure 5). This is not a true oscillatory state, and the amplitude of the fluctuations is small, but this behaviour is certainly interesting. Similar vacillation has been seen as a way for steady convection patterns to lose stability via a Hopf bifurcation (Rucklidge et al., 1993). It is also possible that the observed oscillations are a consequence of the finite geometry, in the sense that the convecton could be interacting with periodic copies of itself. Calculations in larger domains to investigate this further are currently underway.

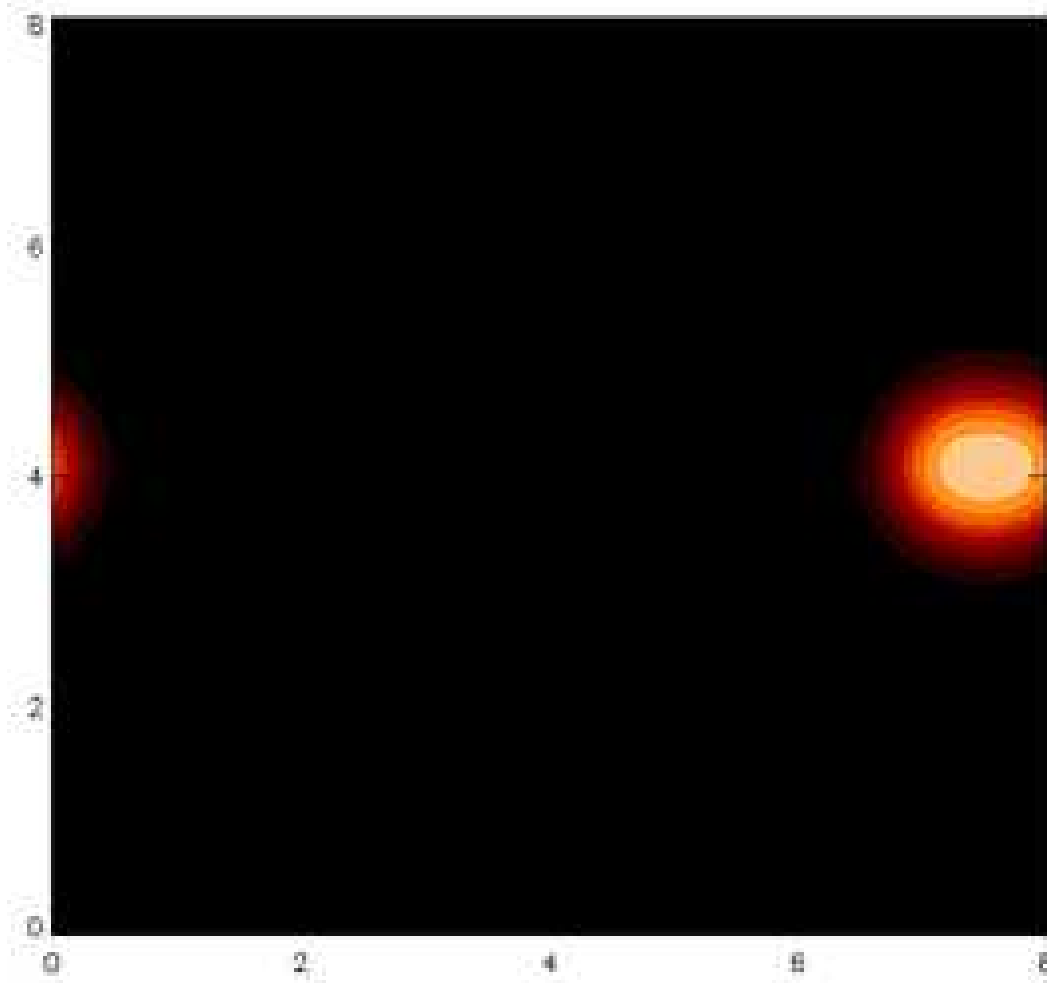


Figure 3: Steady, localised convection at  $Q=215$ . This shows the temperature distribution in a horizontal plane just below the upper surface of the computational domain. Taking into account the periodic boundary conditions, this solution corresponds to a single convective plume. The convecton is close to axisymmetric, but slightly elongated in the  $x$ -direction.

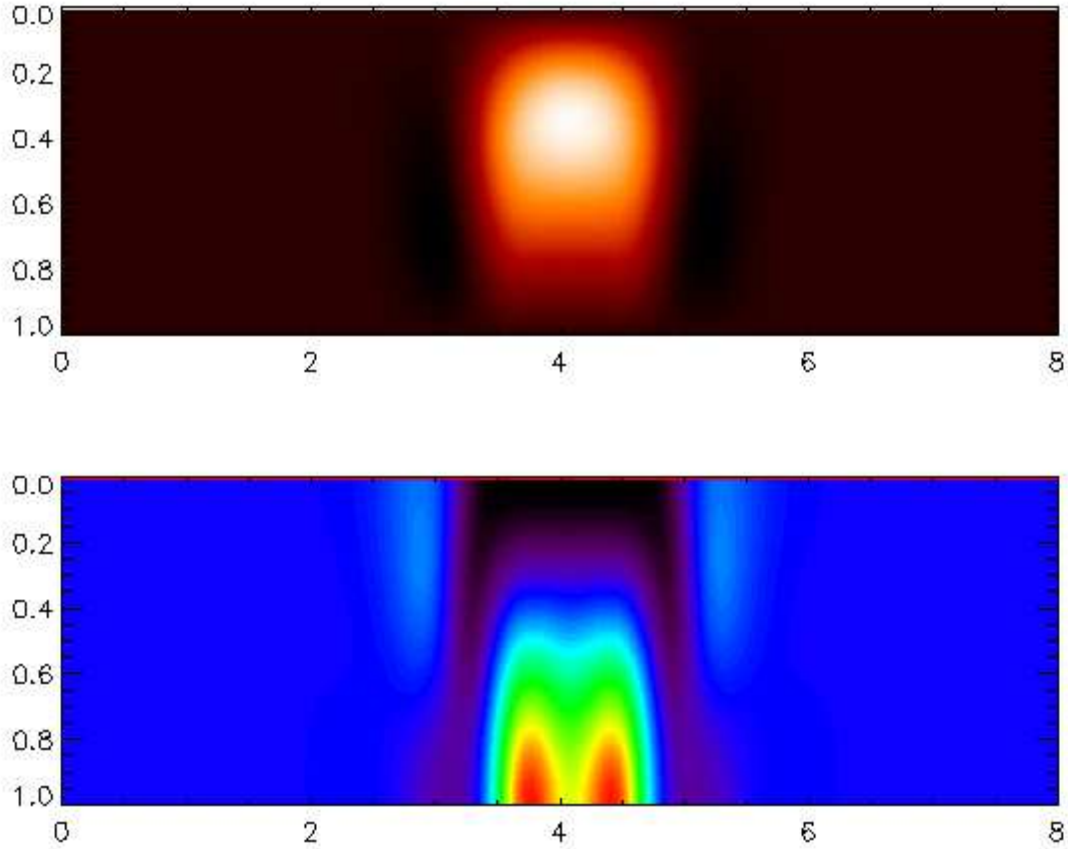


Figure 4: As Figure 3, these plots show snapshots of a convecton at  $Q = 215$ . Top: The perturbation to the background temperature distribution along a vertical slice through  $x = 7.5$ . Contours range from  $-0.11$  (black) to  $0.87$  (white). Bottom: The vertical component of the magnetic field in the same vertical slice. Contours range from  $0.22$  (black) to  $3.67$  (red).



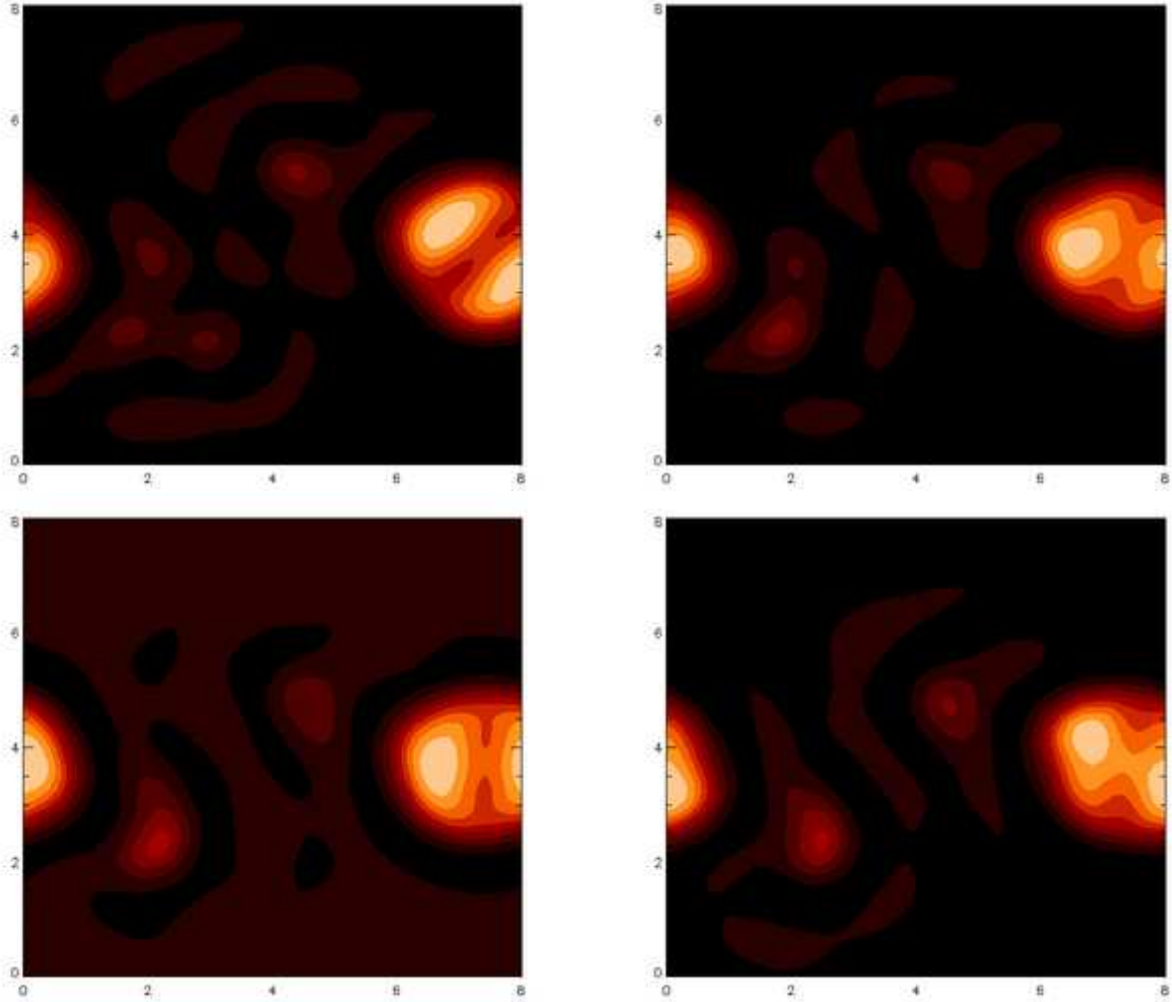


Figure 5: Snapshots of convection along the convection solution branch (at  $Q = 160$ ). These plots show the temperature distribution in a horizontal plane just below the upper surface of the computational domain. These plots are separated by 4.55 time units, the full cycle period is 18.20 time units.

## 4 Discussion and Conclusions

In these numerical simulations we have found strongly localised convective plumes in the subcritical regime of compressible magnetoconvection. These states are not embedded within a background of diffuse weak convection, but rather a static fluid (see figure 3). It is believed that strongly localised, steady states of this type have not previously been observed in three spatial dimensions. Whether umbral dots ever exhibit such an extreme degree of localisation is unclear, but these results do suggest that highly localised plumes could occur if the magnetic fields within sunspot umbrae are strong enough (locally) to produce subcritical conditions for magnetoconvection.

The strongly localised states found in this work are found by continuation of flux-separated states to higher values of  $Q$ . A similar procedure was carried out by Weiss et al. (2002), however, in their work it was found that for sufficiently strong imposed magnetic fields the flux separated solution was lost in favour of small-scale regular convection. Weiss et al. (2002) used the parameter value  $\zeta_0 = 0.2$  whereas in this work  $\zeta_0 = 0.1$ . It is well-known that the value of  $\zeta_0$  controls the near-onset bifurcation structure. Comparison of this work with the findings of Weiss et al. (2002) indicate that it also controls whether or not the solution branch corresponding to flux-separated states continues into the subcritical regime.

Although it is appealing to relate these highly localised convective plumes to umbral dots, one aspect of these solutions that does not compare favourably with umbral dots is that fact that these localised states are steady (or, at best, weakly time-dependent, as shown in Figure 5). So, unlike the observed umbral dots, these solutions do not have finite lifetimes. This may be associated with the simplified nature of the model, which assumes a uniform background state: spatiotemporal inhomogeneities in the umbral background may play an important role in determining the lifetime of an umbral dot. Alternatively, time-dependent behaviour may be the result of interacting plumes. Perhaps the time-dependent state that is shown in Figure 2 is a more realistic representation of the distribution of convective plumes within sunspot umbrae. Work is ongoing to establish whether or not it is possible to find truly localised states that exhibit significant time-dependence. The simplified model of Blanchflower & Weiss (2002) suggests that oscillatory solutions should exist, however, while we cannot rule out this possibility, oscillatory localised states have not yet been observed in the full system of equations.

This model is clearly a highly idealised representation of magnetoconvection within sunspot umbrae. Truly localised states have not yet been found in more realistic models of photospheric magnetoconvection. It would be of great interest to establish whether or not processes such as radiative transfer promote (or inhibit) the formation of strongly localised plumes. It should also be stressed that the range of parameter values that can be considered in numerical models of this type bear little resemblance to true photospheric values (although this is true of all numerical magnetoconvection calculations, regardless of the level of physical complexity). Having said that, we believe that results from models of this type do provide some useful insights into photospheric magnetoconvection.

Magnetoconvection is not the only branch of physics in which strongly localised states are relevant. Similar states have now been found in a variety of other systems, including binary fluid convection (Bergeon & Knobloch, 2008), buckling rod problems, nonlinear optics (Vladimirov et al., 2002) and experiments on a ferrofluid in an applied magnetic field (Richter & Barashenkov, 2005). In a more abstract setting, localised states have also been found in the one-dimensional bistable Swift-Hohenberg equation (Burke & Knobloch, 2006, 2007a,b). The results presented in this paper share many similarities with the behaviour of the Swift-Hohenberg equation in one dimension, as well as the other physical systems mentioned above. There is now a good theoretical understanding of localised states in one extended dimension, however, in higher dimensions the problem is not well understood, and has recently been posed as an open problem (Knobloch, 2008). Having said that, some recent progress has been made. For example, Lloyd et al. (2008) have investigated the properties of spatially localised states in the two-dimensional Swift-Hohenberg equation. In future work, we intend to further explore the relationship between the behaviour of this simple pattern forming system and the magnetoconvection equations.

**Acknowledgements:** This work has been supported by EPSRC grant EP/D032334/1 (SMH) and STFC grant ST/H002332/1. PJB would like to acknowledge the support of STFC. Large-scale computations were performed on the UKMHD Consortium machine based in St. Andrews, UK.

## References

Bergeon A., Knobloch E., 2008, *Phys. Fluids.*, 20, 034102

Bharti L., Beeck B., Schüssler M., 2010, *A&A*, 510, A12

Bharti L., Jain R., Jaaffrey S. N. A., 2007, *ApJ*, 665, L79

Blanchflower S., 1999, *Phys. Lett. A*, 261, 74

Blanchflower S. M., Weiss N. O., 2002, *Phys. Lett. A*, 294, 297

Burke J., Knobloch E., 2006, *Phys. Rev. E*, 73, 056211

Burke J., Knobloch E., 2007a, *Chaos*, 17, 037102

Burke J., Knobloch E., 2007b, *Phys. Lett. A*, 360, 681

Bushby P. J., Houghton S. M., 2005, *MNRAS*, 362, 313

Chandrasekhar S., 1961, *Hydrodynamic and Hydromagnetic Stability*. Dover, New York

Danielson R. E., 1964, *ApJ*, 139, 45

Dawes J. H. P., 2007, *Journal of Fluid Mechanics*, 570, 385

Deinzer W., 1965, *ApJ*, 141, 548

Kitai R., et al., 2007, *PASJ*, 59, S585

Knobloch E., 2008, *Nonlinearity*, 21, T45

Lloyd D. J. B., Sandstede B., Avitabile D., Champneys A. R., 2008, *SIAM Journal on Applied Dynamical Systems*, 7, 1049

Matthews P. C., Proctor M. R. E., Weiss N. O., 1995, *Journal of Fluid Mechanics*, 305, 281

Ortiz A., Rubio L. R. B., van der Voort L. R., 2010, *ApJ*, 713, 1282

Richter R., Barashenkov I. V., 2005, *Phys. Rev. Lett.*, 94, 184503

Rucklidge A. M., Weiss N. O., Brownjohn D. P., Proctor M. R. E., 1993, *Geophys. Astrophys. Fluid Dynamics*, 68, 133

Schüssler M., Vögler A., 2006, *ApJ*, 641, L73

Sobotka M., Bonet J. A., Vazquez M., Hanslmeier A., 1995, *ApJ*, 447, L133

Sobotka M., Brandt P. N., Simon G. W., 1997, *A&A*, 328, 682

Sobotka M., Hanslmeier A., 2005, *A&A*, 442, 323

Socas-Navarro H., Martínez Pillet V., Sobotka M., Vázquez M., 2004, *ApJ*, 614, 448

Tao L., Weiss N. O., Brownjohn D. P., Proctor M. R. E., 1998, *ApJ*, p. L39

Thomas J. H., Weiss N. O., 2008, *Sunspots and Starspots*. Cambridge University Press

Vladimirov A. G., McSloy J. M., Skryabin D. V., Firth W. J., 2002, *Phys. Rev. E*, 65, 046606

Weiss N. O., 1966, *Proc. Roy. Soc. Lond. A*, 293, 310

Weiss N. O., Proctor M. R. E., Brownjohn D. P., 2002, *MNRAS*, 337, 293